
Research Paper

Coupling Between Chemical Reactivity and Structural Relaxation in Pharmaceutical Glasses

Sheri L. Shamblin,^{1,2,3} Bruno C. Hancock,² and Michael J. Pikal¹

Received February 1, 2006; accepted June 5, 2006; published online August 29, 2006

Purpose. To test the hypothesis that the molecular motions associated with chemical degradation in glassy amorphous systems are governed by the molecular motions associated with structural relaxation. The extent to which a chemical process is linked to the motions associated with structural relaxation will depend on the nature of the chemical process and molecular motion requirements (e.g., translation of a complete molecule, rotational diffusion of a chemical functional group). In this study the chemical degradation and molecular mobility were measured in model systems to assess the degree of coupling between chemical reactivity and structural relaxation. The model systems included pure amorphous cephalosporin drugs, and amorphous molecular mixtures containing a chemically labile drug and an additive expected to moderate molecular mobility.

Methods. Amorphous drugs and mixtures with additives were prepared by lyophilization from aqueous solution. The physical properties of the model systems were characterized using optical microscopy and differential scanning calorimetry. The chemical degradation of the drugs alone and in mixtures with additives was measured using high-performance liquid chromatography (HPLC). Molecular mobility was measured using isothermal microcalorimetry to measure enthalpy changes associated with structural relaxation below T_g .

Results. A weak correlation between the rates of degradation and structural relaxation times in pure amorphous cephalosporins suggests that reactivity in these systems is coupled to molecular motions in the glassy state. However, when sucrose was added to one of the cephalosporin drugs stability improved even though this addition reduced T_g and the relaxation time constant, τ_D^β , suggesting that there was no correlation between reactivity and structural relaxation in the cephalosporin mixtures. In contrast, the rate of ethacrynate sodium dimer formation in mixtures was more strongly coupled to the relaxation time constant, τ_D^β .

Conclusions. These studies suggest that the extent to which chemical degradation is coupled to structural relaxation in glasses motions is determined by how closely the motions of the rate controlling step in chemical degradation are associated with structural relaxation. Moderate coupling between the rate of dimer formation for ethacrynate sodium in mixtures with sucrose, trehalose and PVP and structural relaxation constants suggests that chemical changes that require more significant molecular motion, and includes at least some translational diffusion, are more strongly coupled to the molecular motions associated with structural relaxation. The observation that sucrose stabilizes cefoxitin sodium even though it lowers T_g and reduces the relaxation time constant, τ_D^β is perhaps a result of the importance of other kinds of molecular motions in determining the chemical reactivity in glasses.

KEY WORDS: amorphous; coupling; glass; molecular mobility; relaxation time constant; structural relaxation.

INTRODUCTION

It is well recognized that chemical reactions that occur in the solid state require some degree of molecular mobility. In crystalline solids, chemical reactions are believed to both initiate and propagate in regions where crystal defects are concentrated or where there are high degrees of molecular

disorder. It is the less restricted molecular motion in regions of higher disorder that facilitates chemical reactivity. This hypothesis is supported by observations that chemical degradation is significantly higher in amorphous drugs in comparison to the analogous crystal form (1,2).

Since the degree of molecular mobility is likely to play a critical role in the chemical stability of pharmaceutical dosage forms, both crystalline and amorphous, the relationship between chemical reactivity and molecular motion is an area of great interest. While there are many examples of well-characterized chemical reactions that take place in the amorphous state (1–3), and studies that have measured or characterized molecular mobility in the amorphous drugs and excipients (4–6), the link

¹ Department of Pharmaceutical Sciences, School of Pharmacy, University of Connecticut, Storrs, CT 06269, USA.

² Groton Laboratories, Pfizer Inc., Groton, CT 06340, USA.

³ To whom correspondence should be addressed. (e-mail: sheri.l.shamblin@pfizer.com)

between chemical reactivity and molecular mobility in pharmaceutical solids is still poorly understood.

In most examples from the literature that have examined the importance of molecular mobility to chemical reactivity in an amorphous system, the glass transition temperature (T_g) has been used as a measure of molecular mobility. The T_g offers the benefit of being experimentally accessible by differential scanning calorimetry and is well recognized as the temperature where viscosity and relaxation time are on the order of 10^{10} – 10^{13} Pa s and 100 s, respectively. In some cases the degree of chemical reactivity can clearly be correlated to molecular motion as measured by the glass transition temperature (7–9); in other documented examples the chemical stability cannot be directly correlated to the T_g (7,10–12). One such example that illustrates the often observed discrepancies regarding the relevance of T_g to chemical reactivity is the rate of deamidation for a peptide that was well correlated to T_g when formulated in matrices containing poly(vinylpyrrolidone), but not when the matrices contained poly(vinylalcohol) (7).

One possible explanation for the absence of a general correlation between chemical reactivity and T_g is that the T_g alone does not accurately account for the complex dependence of molecular motions on temperature in supercooled liquids and glasses (13,14). In particular, the T_g is only one measure of molecular mobility over a narrow range of temperatures. Measurements of viscosity and relaxation times in glasses and supercooled liquids over wider ranges in temperature have shown that the temperature dependence of molecular mobility can vary greatly for different materials (15). Therefore, direct measures of mobility at the temperatures where chemical degradation takes place may be more appropriate than using T_g (or the temperature relative to T_g) to correlate chemical stability to molecular mobility.

The measurement of viscosity in supercooled liquids is frequently used as a measure of molecular mobility in glasses and liquids using the Stokes–Einstein relation that relates the translational diffusion coefficient, D , at a given temperature T , to viscosity, η by the equation,

$$D = \frac{kT}{6\pi\eta a} \quad (1)$$

where a is the hydrodynamic radius of the diffusing species and k is the Boltzmann constant. The diffusion process characterized by D also has a characteristic or ‘jump’ distance of length, l , and a characteristic time for diffusion, τ . At T_g , where the viscosity is typically 10^{10} – 10^{13} Pa s, the characteristic diffusion path, l , is ~ 0.2 Å and the characteristic diffusion time, τ , is ~ 200 s (15). Invoking the Einstein equation, the diffusion coefficient and relaxation time are inversely related relaxation time by the equation,

$$D = \frac{l^2}{\tau} \quad (2)$$

where, D , l and τ are defined in the same way as above. The relationship in Eq. 2 can describe structural relaxation in glasses if it is assumed molecular rearrangements that lead to structural relaxation in glasses can be described by series of diffusional jumps described by length l , that occur in a characteristic time, τ (16). Likewise, the molecular motions that lead to a chemical process that requires diffusion can be described in terms of viscosity (15–17). If it is further assumed that molecular motions responsible for both structural relaxation and chemical

instability are perfectly coupled to viscosity, chemical instability can be coupled directly to the structural relaxation process. In such a case the temperature dependence of the two processes would be the same and the chemical reaction rate constant, k_c , can be related to the characteristic time constant for structural rearrangement, τ_s through the diffusion coefficient and viscosity by Eq. 3.

$$\frac{k_{c2}}{k_{c1}} \approx \frac{D_2}{D_1} \approx \left(\frac{T_2}{T_1}\right) \left(\frac{\tau_1}{\tau_2}\right)^c \quad (3)$$

The value of c , a coupling factor introduced to compensate for differences in the diffusion coefficients (and diffusion length) for chemical and structural relaxation processes (16–18), is unity when coupling between chemical and physical processes is perfect. In most cases, the molecular motions for chemical and physical process are not likely to be perfectly coupled and the value of c will be less than unity (16). For example, electrical conductivity was shown to have a temperature dependence that is significantly different than viscosity, an indication electrical conductivity is decoupled from viscosity (19,20). The complete decoupling of small-molecule diffusion in glassy polymers from structural relaxation (20) is another example of decoupling of motions responsible for different physical processes within the same system. One example of nearly complete coupling is the observation that the T_g value obtained by measuring the internal motions of a globular protein in a glycerol matrix (measured by FTIR) differs only slightly from the T_g measured on the bulk system by DSC (21).

Several examples in the literature compare the chemical degradation rate in the glassy state to structural relaxation rates with different conclusions regarding the correlation between chemical degradation and structural relaxation. When lysozyme was colyophilized with sucrose or trehalose, the aggregation rate, which is not strictly speaking a true chemical process, was roughly correlated with structural relaxation times measured using a differential scanning calorimetry (22). Zograf and coworkers have reported an example of a strong correlation between the rates of cyclization and predicted structural relaxation times of a small-molecule drug below T_g using the well studied amorphous quinapril hydrochloride system (17). More recently Chang *et al.* have reported deamidation rates (and aggregation rates) in an IgG1 antibody did correlate to relaxation time constants over part of the composition range of mixtures containing protein and sucrose, but not over the entire range investigated (10). No other studies have examined the importance of the nature of the chemical reaction and coupling to structural relaxation in glasses.

The general aim of this work is to further examine the coupling between chemical degradation and molecular mobility in glassy pharmaceutical systems. Specifically we will be studying the role of drug degradation mechanism and the influence of miscible excipients that are added to moderate the degree molecular mobility in coupling of chemical degradation to molecular mobility. This coupling will be quantified using mathematical relationships in the following equations,

$$\log \tau_c = c \log \tau_s \quad (4)$$

or

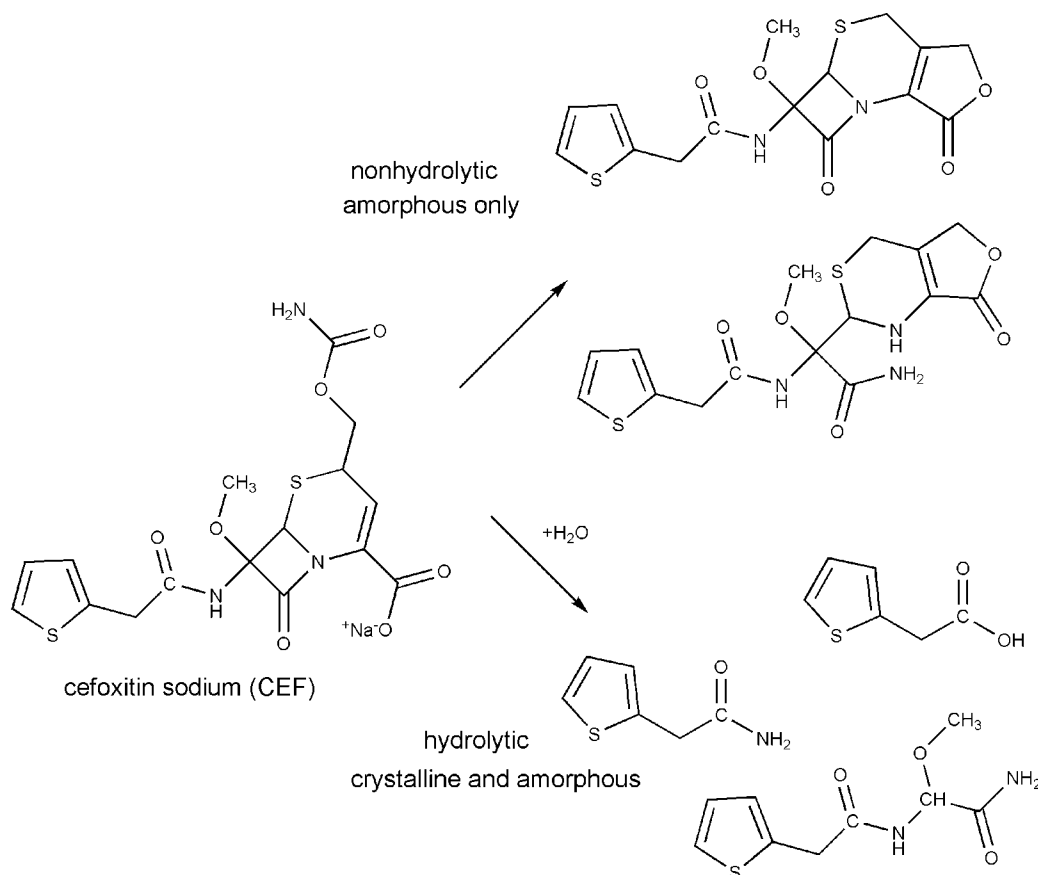
$$\log \frac{1}{k_c} = c \log \tau_s \quad (5)$$

where τ_c and τ_s are time constants that characterizes motions contributing to chemical change and structural relaxation, respectively, and c is the 'coupling' constant, defined in Eq. 3, that accounts for differences in the fundamental motions that contribute to the chemical and structural changes. In Eq. 5, τ_c is approximated by the reciprocal of the rate of chemical degradation, k_c . The coupling between chemical degradation and molecular motions associated with structural relaxation is expected to depend on the nature of the chemical process and the molecular motions requirements (e.g., translation of a complete molecule, rotational diffusion of a chemical functional group). The extent to which the configurational requirements for chemical change are different from those needed for structural relaxation will be reflected in deviations of the coupling constant, c , from unity.

Coupling between chemical change and the molecular mobility is tested in this study using chemical degradation

and structural relaxation data previously reported in the literature for two amorphous cephalosporin drugs (2). The thermal data acquired using a highly sensitive isothermal calorimeter previously reported for cefamandole and cephalothin (2) contains both chemical degradation and structural relaxation data; however at that time it was not possible to deconvolute these two processes. Now, following the work of Liu *et al.*, it is possible to separate the thermal effects of the two processes and therefore, to extract information about the chemical degradation and structural relaxation from the thermal data (23). In addition, we study the chemical reactivity and structural relaxation of two other chemically labile amorphous drugs, cefoxitin sodium (CEF) and ethacrynate sodium (ECA). The reaction pathways for CEF and ECA are shown in Fig. 1. The mechanisms for chemical degradation for the two amorphous drugs differ considerably, which allows an investigation of the importance of the type of

a.



b.

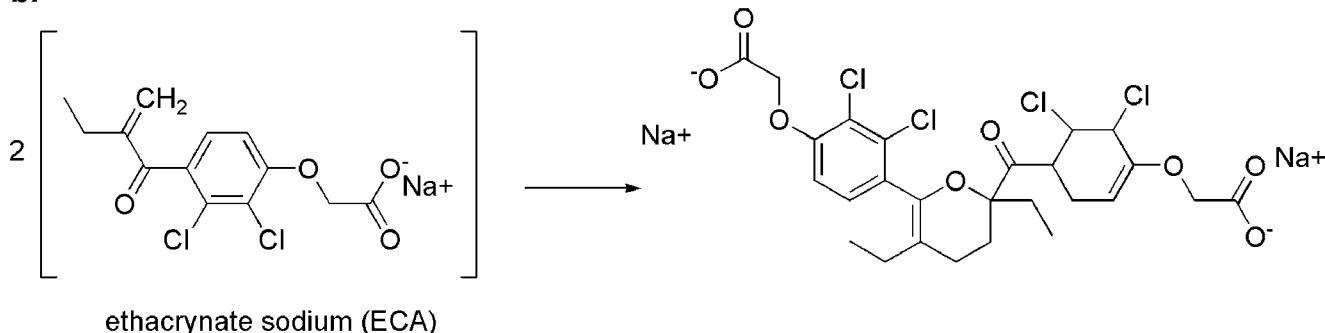


Fig. 1. Degradation mechanisms for (a) cefoxitin sodium adapted from (1,25) and (b) ethacrynate sodium (24).

degradation mechanism in determining coupling to structural relaxation. In the amorphous state the dimer of ECA is formed via a Diels–Alder condensation while amorphous CEF can degrade via hydrolytic ring opening of the β -lactam ring and non-hydrolytic formation of lactone and acid lactone species (1,24,25). Since the mobility requirements (i.e., length of the diffusion pathway) for ECA dimerization *versus* the ring opening and ring closure processes are expected to be different, the degree of coupling between chemical reactivity and glass dynamics for these two drugs is expected to be somewhat different. In general, the coupling coefficient for the process involving the longer (molecular) length parameter, expected to be the dimerization reaction in this study, should be larger. The effect of excipients on the coupling of chemical change to structural relaxation was tested in this study by preparing molecular mixtures of two model drugs with sugars (sucrose and trehalose) or a polymer, poly(vinylpyrrolidone) (PVP) by lyophilization of their aqueous solutions. These additives were chosen to produce differences in molecular mobility in drug mixtures at a given additive concentration. The reactivity of the amorphous drugs alone or in mixtures was measured using high-performance liquid chromatography (HPLC) to monitor the composition of the drug and degradants with time. The degree of molecular mobility was measured using an isothermal microcalorimeter to directly measure the enthalpy loss associated structural relaxation. When possible the enthalpy relaxation and chemical degradation were measured simultaneously on the same sample.

EXPERIMENTAL

Materials

Cefoxitin sodium (Merck), trehalose (Sigma), sucrose (Fisher), poly(vinylpyrrolidone)(PVP) K12 (BASF) and were used as received. Crystalline ethacrynic acid (Sigma) was used as received to generate ethacrynate sodium in solution. The amorphous forms of cefoxitin sodium, ethacrynate sodium, sucrose and trehalose and various amorphous mixtures were prepared by lyophilization of aqueous solutions containing one or more components.

Methods

Preparation of Amorphous Materials by Lyophilization

The preparation of amorphous cephalothin sodium and cefamandole sodium by lyophilization from aqueous solutions was described previously (2). Amorphous cefoxitin sodium was prepared by lyophilization of an aqueous solution containing 5% *w/v* cefoxitin sodium. Mixtures containing CEF were prepared by combining stock solutions of CEF with sucrose, trehalose or PVP K12. The combined concentration of drug and excipient in the aqueous solution was 5% *w/v*. Once freeze-dried the ratios of drug to excipient in these mixtures was equal to 1:3 and 1:10.

Ethacrynate sodium was formed in aqueous solution by titration of the free acid with a 0.1 N NaOH solution. Sodium hydroxide solution was added very slowly in order to maintain

a local pH less than 9.0 and minimize the degradation of the drug in solution. The final pH of the drug solutions ranged from pH 7.1–7.3 after the addition of a slight excess of hydroxide ion. Aqueous solutions containing only ECA at a concentration 2.0% *w/v* were lyophilized in an attempt to produce amorphous ECA. The ECA mixtures were prepared by adding the second component to a stock drug solution to give drug:excipient ratios of 1:10 and 1:3. The combined concentration of drug and excipient in these solutions was 5%.

Aqueous solutions containing drug alone and drug and excipient were freeze-dried using a DuraStop Tray Dryer with a (FTS Systems, Stone Ridge, NY, USA) microprocessor. Primary drying was carried out below the T_g' of the drug and various excipients by setting the shelf temperature to -25°C with a chamber pressure of 100 mTorr. In general, the product temperatures were $-35 \pm 1^\circ\text{C}$ throughout primary drying. Secondary drying was performed for 4 h at 0°C , and then at 40°C for 6 h. The samples were cooled to 0°C and sealed under vacuum. The samples were stored at -23°C until they were analyzed or placed on stability.

The water contents of freeze-dried mixtures were determined to be $0.3\text{--}0.6 \pm 0.2\%$ using the Karl–Fischer titration method. The freeze-dried samples were confirmed to be amorphous using optical light microscopy to look for the presence of birefringence which would signal crystallinity.

Measurement of T_g of Amorphous Materials and their Mixtures

The glass transition temperatures of the freeze-dried materials were determined using differential scanning calorimetry to detect the change in heat capacity associated with T_g . A Model 2920 DSC (TA Instruments, New Castle, DE, USA), was used in the standard mode at a heating rate of $10^\circ\text{C}/\text{minute}$ to measure T_g . Prior to this measurement, all materials were first heated through T_g , and then cooled at $20^\circ\text{C}/\text{min}$ to give the materials a similar thermal history. The reported T_g values correspond to the maximum of the first derivative of the heat flow curve as a function of temperature, which is often referred to as the 'midpoint' T_g .

Chemical Degradation of Model Amorphous Drugs Using High Performance Liquid Chromatography

High performance liquid chromatography was used to monitor the stability of CEF alone and in mixtures. The HPLC assay used to monitor the stability of CEF under various conditions consisted of a mobile phase of 1% aqueous acetic acid buffer solution (90% *v/v*) and acetonitrile (10%), an injection volume of 10 μl , a Vydac C18 (HTS-0546) column with a flow rate of 1.0 ml/min. A UV detector with a wavelength of 210 nm was used in order to quantitatively measure drug concentration and to confirm the formation of the primary degradation products formed by rupture of the β -lactam ring. CEF concentration as a function of time was determined using a standard stock drug solution to produce a standard response curve with an RSD that was $<1\%$. The

concentration of CEF remaining was determined by the analysis of three separate samples with at least two replicated measures for each. The relative standard deviation associated with the stability samples was less than 3%.

For ECA, a gradient HPLC assay was used to measure the drug concentration and for a qualitative assessment of the degradation peaks. The injection volume was 15 μl , the column was a Vydac Targa C18 (TS 0546-C185) and a wavelength of 280 nm was used to detect the drug and degradants. Initially the mobile phase was a mixture of methanol (45% v/v) and 0.05 M sodium phosphate buffer with a pH of 5.6 (55% v/v), which was combined with a flow rate of 1.5 ml/min, to detect the drug, which eluted around 4 min. In order to detect the primary degradation product, which is a dimer of the drug, the ratio of methanol to phosphate buffer was slowly increased to 50% methanol and 50% phosphate buffer and the flow rate was decreased to 1.0 ml/min. Drug concentration as a function of time was determined using a standard stock drug solution to produce a standard response curve with an RSD that was <1%. The concentration of drug remaining was determined using three separate samples with at least two replicated measures for each. The relative standard deviation associated with the stability samples was less than 2%.

Measurement of Structural Relaxation and Chemical Reactivity Using Isothermal Microcalorimetry

The exothermic heat associated with the structural relaxation was measured isothermally using a Thermal Activity Monitor (TAM) (Model 2277, Thermometric, Sweden) microcalorimeter. The thermal data were used to determine rates of structural relaxation of the excipients that were combined with the drugs at the temperatures drug stability was studied, for those model drugs that could be isolated in the amorphous form in the absence of excipients and in selected the drug-containing mixtures.

The calorimetric experiments were performed using about 300 mg of sample contained in stainless steel ampoules fitted with water-tight gaskets. The freeze-dried samples were transferred from storage vials to the measuring ampoules in a low humidity (<2% RH) glove bag to prevent the absorption of water vapor. A sample of crystalline glycine of equivalent weight in a stainless steel ampoule was used as a thermally inert reference. The microcalorimeter was calibrated at each temperature using a 300 μW electrical signal as recommended by the manufacturer. The sample and reference ampoules were placed in the equilibrated position in the calorimeter for 30 min, and then slowly lowered into the measurement position. The power output was recorded as a function of time every 3 min for up to 90 h. The data corresponding to the first 30 min that the sample and reference were in the measurement position were discarded due to artifacts associated with equilibration of the ampoules in sample and reference chambers. A minimum of two samples were tested at any given set of experimental conditions.

Calculation of Structural Relaxation Times Using Differential Scanning Calorimetry

Relaxation times at different temperatures from those directly measured using isothermal microcalorimetry at a

reference temperature were determined by use of the relationship between relaxation time and temperature (26),

$$\left(\frac{d \ln \tau}{d(T/T_g)} \right)_{T_g} = - \frac{C}{(\Delta T_g/T_g)} \left(1 - \gamma \left(1 - \frac{36.9 \cdot \beta}{C} \cdot \frac{\Delta T_g}{T_g} \right) \right) \quad (6)$$

where ΔT_g is the width of the glass transition region, τ is the relaxation time and β is the 'stretched' exponent in the Kohlrausch–Williams–Watts equation and C is a constant related to the methodology for determining the width of the glass transition. The term γ is related to the 'excess' or configurational heat capacity in the glass,

$$\gamma = \frac{C_p^l - C_p^g}{C_p^l - C_p^{xstat}} = \frac{\Delta C_p}{C_p^l - C_p^{xstat}} \quad (7)$$

Eq. 7 is the defining equation of γ , but γ was calculated from the heat capacity changes at T_g , ΔC_p , using an empirical expression that is a useful approximation (26). Equation 6 was shown to be an approximation with useful accuracy for predicting relaxation times when using the assumption that all systems have the same relaxation time at their glass transition temperatures (26). This assumption was not needed in this study since experimental relaxation time data at 50°C were available. The values of β used in the estimation of the temperature dependence of structural relaxation times were taken to be those values previously reported for the pure excipients (26). These values were estimated from the DSC overshoot peaks as described in the reference and were 0.46 (sucrose), 0.48 (trehalose), and 0.41 (PVP). Thus, we simply use Eq. 6 to determine the temperature dependence of the relaxation time and thereby obtain relaxation time data at 60 and 70°C from integration of Eq. 6 between 50°C and the appropriate higher temperature.

Characterization of Physical Form Using Optical Microscopy

Optical microscopy was used to confirm the amorphous character of model systems following preparation of samples by lyophilization, samples subjected to elevated temperatures for chemical stability studies, and samples analyzed using isothermal microcalorimetry to measure structural relaxation and/or chemical stability. The absence of birefringence was taken as an indication of amorphous content. Analysis was based on three separate samples taken from three different locations.

FT-Raman Spectroscopy

FT-Raman spectra were collected on a Perkin-Elmer System 2000 instrument with a near infrared Nd:YAG laser operating at 1064 nm. The laser power was typically 800 mW at the sample and an InGaAs detector was used. Back-scattered radiation at an angle of 180°C was collected and the Stokes radiation reported. Indene was used as a reference standard to monitor wavenumber accuracy. Five hundred twelve scans at a resolution of 4 cm^{-1} were averaged for each sample. Samples were analyzed in NMR tubes (5-mm outer diameter) with continuous rotation.

RESULTS

Chemical Reactivity and Structural Relaxation in Amorphous Cephalothin Sodium and Cefamandole Sodium

The relationship between chemical reactivity and mobility was first tested in two, single-component systems by further analyzing previously reported thermal data for cephalothin sodium and cefamandole sodium (2). The thermal data, shown in Fig. 2, were collected using a highly sensitive microcalorimeter and are qualitatively similar for both drugs. Initially these samples have a high thermal activity that decreases sharply over several hours to eventually approach an apparent constant thermal activity. The thermal activity at longer times (>24 h), in significant part, reflects the rate of chemical degradation, and as reported previously, degradation was confirmed using HPLC to monitor the sample purity (2). The initially high thermal activity that decreases rapidly over the early part of the study is attributed mostly to the loss in enthalpy due to structural relaxation of the glasses.

The chemical degradation rates and structural relaxation time constants for cephalothin sodium and cefamandole sodium at 40°C were determined using the Modified Stretched Exponential (MSE) equation. The MSE equation has been used to describe relaxation behavior measured using NMR (27) and was recently applied to structural relaxation in glasses (2,23). This equation (Eq. 8) has the form of a 'stretched' exponential equation and is used to describe relaxation behavior that is not exponential and therefore cannot be described by a single relaxation time constant. The MSE equation offers a numerical advantage over the more commonly used Kohlraush–Williams–Watts equation (KWW) equation in that it avoids the problem of infinite initial relaxation rate at time-zero that is characteristic of the derivative of the KWW enthalpy relaxation equation.

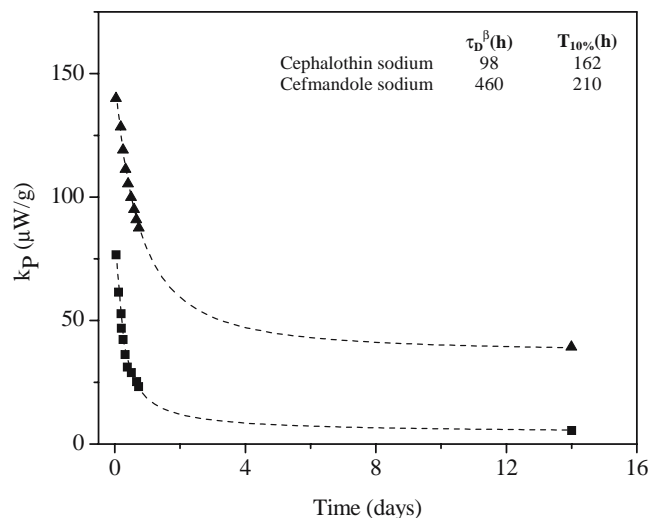


Fig. 2. Isothermal calorimetry data for the cefamandole sodium (■) and cephalothin sodium (▲) at 40°C. Dashed lines represent 'best fit' line using modified stretched exponential equation. The relaxation times and times required for 10% degradation, $T_{10\%}$ (h), are given in the table in the inset.

The MSE can be used to describe the enthalpy changes associated with structural relaxation in glasses at a particular temperature $\Delta H(T, t)$, using the relaxation time constants τ_0 and τ_1 and the stretched exponential constant, β . The relaxation time constants τ_0 and τ_1 are relaxation constants reflecting short and long time behavior, respectively. The characteristic, non-exponential relaxation behavior is usually attributed to a distribution of relaxation times in which case β reflects a distribution of relaxation times and is therefore less than 1 (i.e., $0 < \beta < 1$).

$$\Delta H(T, t) = \Delta H_\infty(T) \left(1 + \exp \left(- \left(\frac{t}{\tau_0} \right) \left(1 + \frac{t}{\tau_1} \right)^{(\beta-1)} \right) \right) \quad (8)$$

The term ΔH_∞ is the total enthalpy change required for the glass to become fully relaxed and depends on temperature. The ΔH_∞ can be estimated at particular temperature using Eq. 9,

$$\Delta H_\infty = \Delta C_p (T - T_g) \quad (9)$$

where ΔC_p is the change in heat capacity observed at the glass transition (T_g) and can be measured using DSC.

Since three relaxation constants τ_0 , τ_1 and β , in the MSE equation are required to describe the relaxation process all three time constants should be taken into consideration in the characterization of relaxation behavior in glasses (28). Liu and Pikal have advocated the use of a single 'stretched relaxation time' parameter, τ_D^β , for the characterization of relaxation behavior in pharmaceutical glasses that incorporates the relaxation constants τ_0 , τ_1 and β (23). The relationship between τ_D^β and the relaxation time constants, τ_0 , τ_1 and β is shown in Eq. 5 below.

$$\tau_D^\beta = \tau_0^{\left(\frac{1}{\beta}\right)} \tau_1^{\frac{(\beta-1)}{\beta}} \quad (10)$$

Note that the MSE equation reduces to the same form of the KWW equation at long times, where τ_D^β , becomes equivalent to the value of τ in the KWW equation. Thus τ_D^β is the MSE equivalent of the relaxation time, τ in the KWW equation.

Structural relaxation time constants can be obtained from the thermal data acquired using a microcalorimeter, by taking the first derivative the MSE (Eq. 10) with respect to time to give the power P (dH/dt) as,

$$P = 277.8 \frac{\Delta H_\infty}{\tau_0} \left(1 + \frac{\beta t}{\tau_1} \right) \left(1 + \frac{t}{\tau_1} \right)^{(\beta-2)} \exp \left[- \left(\frac{t}{\tau_0} \right) \left(1 + \frac{t}{\tau_1} \right)^{(\beta-1)} \right] \quad (11)$$

For those systems in which the thermal activity can be attributed only to structural relaxation, Eq. 11 can be used to obtain the relaxation time constants. However, for both of the cephalosporins the observed thermal activity also reflects the exothermic process of chemical degradation, which can be significant. In this case, the overall power (P_{total}) can be

expressed as a sum of power due to enthalpy relaxation (Eq. 11) and chemical degradation, P_k with the equation,

$$P_{\text{total}} = 277.8 \frac{\Delta H_{\infty}}{\tau_0} \left(1 + \frac{\beta t}{\tau_1}\right) \left(1 + \frac{t}{\tau_1}\right)^{(\beta-2)} \exp \left[-\left(\frac{t}{\tau_0}\right) \left(1 + \frac{t}{\tau_1}\right)^{(\beta-1)} \right] + P_k \quad (12)$$

Strictly speaking the P_k term, which reflects the rate of chemical degradation, is not exactly independent of time as suggested in Eq. 12 since chemical degradation rates typically show 'square-root' time kinetics. However, the structural relaxation data can be obtained over a time-scale that is very short for most chemical reactions, the reaction rate is effectively constant over the time period of the relaxation time measurement, and the value of P_k is effectively constant.

To investigate the relationship between the rate of chemical degradation and the rate of structural relaxation in the two cephalosporin drugs, the thermal activity data shown in Fig. 2 were analyzed using Eq. 12. A least-squares method was used to obtain the relaxation time constants τ_0 , τ_1 and β and P_k values that best describe the data. The molecular mobility for the two drugs at 40°C was determined using a single relaxation time constant, τ_D^{β} , a convention that was previously reported in the literature. The value of τ_D^{β} is inversely related to rate of structural relaxation and degree of molecular mobility; thus a decrease in τ_D^{β} suggests faster structural relaxation and a greater degree of molecular mobility. The rate of chemical degradation was compared to the τ_D^{β} values using the times required for 10% degradation, $T_{10\%}$ that were determined based on the chemical degradation rates that were obtained using HPLC and were reported previously (2). The $T_{10\%}$ and τ_D^{β} values are compared for the two drugs in the table inset in Fig. 2. The longer relaxation time constant for cefamandole sodium indicates a lesser degree of molecular mobility as compared to cephalothin sodium. Cefamandole sodium also shows a longer $T_{10\%}$, indicating a slower rate of chemical degradation than cephalothin sodium. Thus, these data suggest significant coupling between the chemical degradation and rate of structural relaxation processes in these two cephalosporin drugs. The degree of coupling will be discussed further in the discussion section of this manuscript.

Cefoxitin Sodium (CEF) Chemical Stability

The physical form of cefoxitin sodium lyophilized samples of the drug alone and in mixtures with sucrose, trehalose or PVP at ratios of 1:3 and 1:10 drug was confirmed to be amorphous using optical light microscopy to confirm the absence of birefringence. All of the mixtures showed a single glass transition temperature indicating that CEF was miscible with sucrose and PVP. Due to the close proximity of the T_g of CEF (127°C) to that of trehalose (114°C), a single T_g for the mixture with trehalose could not be interpreted unequivocally to mean the two components were miscible. However the width of the T_g and the change in heat capacity at T_g were similar in value to those for the sucrose mixtures, strongly suggesting the CEF mixture containing trehalose is composed of a single amorphous phase.

Storage of CEF alone and in mixtures containing sucrose and trehalose at elevated temperatures resulted in loss in potency of CEF. In these samples the loss in CEF potency was accompanied by the formation the same four degradation peaks in the HPLC chromatogram, and several very minor peaks that could not be resolved. CEF is known to have multiple degradation pathways in the solid and solution states (1,25,29). In crystalline CEF, the primary degradation pathway is hydrolysis where the rate and extent of degradation limited by the presence of water. In the amorphous state CEF degrades via hydrolysis and nonhydrolytic pathways that are not seen the crystalline form, presumably because of a lesser degree of molecular mobility. Based on the number of degradation peaks and the retention times of the four primary degradation peaks relative to that for the main drug peak it appears amorphous CEF degrades via both the hydrolytic ring-opening of the β -lactam ring and the non-hydrolytic degradation pathways to the lactone and lactone acid, as shown in Fig. 1.

In the mixtures containing PVP, significant degradation was observed immediately following preparation by freeze-drying. Degradation continued to proceed rapidly in these mixtures even at ambient temperatures where the amorphous drug alone and in the other mixtures was stable for several months. Several peaks were observed in HPLC chromatograms for the CEF-PVP mixtures that were not seen in mixtures containing sucrose or trehalose suggesting that additional degradation pathways occur in the presence of PVP. The mechanism for the enhancement in chemical reactivity of cefoxitin sodium in mixtures with PVP is not known. However, since the influence of PVP on the chemical stability of CEF is anomalous, and obviously not related to its effect on molecular mobility alone, the mixtures with PVP were not further characterized.

The rate of CEF degradation alone and in mixtures with sucrose and trehalose was determined based on the loss of peak area of the drug due to the large number of degradant peaks and the close proximity of these peaks to one another in the HPLC chromatograms. The degradation rate of CEF alone and in mixtures with sucrose and trehalose at 40 and 50°C increased with temperature as expected and was essentially constant over time. The physical stability of the amorphous drug alone and in the mixtures was maintained during the chemical degradation studies as confirmed by the absence of birefringence in stability samples.

In the presence of sucrose the rate of degradation of the drug decreased, whereas when mixed with trehalose, the reactivity of the drug was nearly unchanged. These observations are illustrated in Fig. 3, where the fraction of drug remaining following storage at 40°C is plotted *versus* time for the drug alone and in the 1:3 mixtures. The chemical degradation rates that were measured for amorphous cefoxitin alone and in the all of the mixtures using HPLC are reported in Table I as the time required for 10% degradation, $T_{10\%}$. Although stability is improved by the presence of sucrose, the degradation rate is still much faster than the crystalline drug (1). At both temperatures there appeared to be no large effect of sucrose or trehalose concentration (i.e., only a small difference when comparing the 1:3 and the 1:10 mixtures). Typically degradation rates in glasses are not constant over long times, but rather can normally be

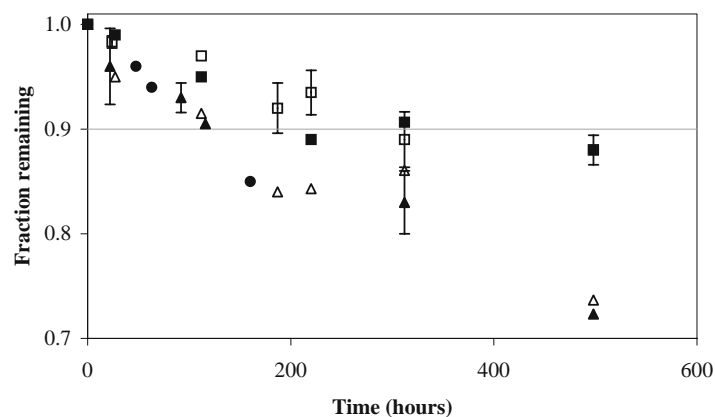


Fig. 3. Fraction of CEF remaining following storage alone (●) and in mixtures with sucrose 1:10 (□), 1:3 (■) and trehalose, 1:10 (△); 1:3 (▲) at 40°C.

described using stretched time kinetics (i.e., the degradation is linear when plotted *versus* square-root of time). In these studies it was noted that there was some transfer of moisture from the stopper, which would have caused acceleration of the reaction with increasing time. That is, increasing moisture content with time may have offset the decrease in degradation rate with increasing time that is normally observed in glassy pharmaceuticals, thus producing a net result of apparent ‘zero-order’ kinetics. Since only the initial degradation rates were of interest in this study, initial rates or $T_{10\%}$ data are reported (i.e., excessive degradation changes the physical and chemical properties of the system thereby complicating interpretation of the results).

Molecular Mobility in Cefoxitin Systems

Molecular mobility in the cefoxitin systems at different temperatures alone and in mixtures may be compared by considering the relative glass transition temperatures, or better as measured using stretched enthalpy relaxation time constants (τ_D^β). The T_g values of CEF and each of the additives shown in Table II suggests that sucrose should increase the molecular mobility of CEF significantly, while trehalose would impart only a slight increase in mobility. The much smaller value of τ_D^β value for pure sucrose, relative to trehalose, in Table III confirms that the molecular mobility in sucrose is much greater than in trehalose at 40 and 50°C. Thus, assuming the chemical reactivity is linked to the structural

Table I. Summary of Time Required for 10% Degradation ($T_{10\%}$) and the Relaxation Time Constants at 40°C and 50°C for CEF Alone and in Mixtures with Sucrose and Trehalose

	$T_{10\%}$ (h) HPLC		τ_D^β (h) TAM	
	40°C	50°C	40°C	50°C
CEF	110	20	39 (20)	29 (2.0)
CEF:sucrose 1:10	380	60	28 (0)	7 (3)
CEF:sucrose 1:3	250	45	22 (0.0)	6.4 (0.1)
CEF:trehalose 1:10	150	20	97 (11)	19 (0.6)
CEF:trehalose 1:3	120	18	105 (4.0)	20 (0.1)

The standard deviation in τ_D^β is shown in parenthesis next to each value of τ_D^β .

relaxation rate, it is expected that sucrose would increase the rate of chemical degradation of CEF while trehalose would have little effect on the rate of degradation (30).

Despite a lowering of T_g , trehalose did slightly increase the stability of CEF. Even more surprising was the stabilizing effect of sucrose on CEF, in spite of a large reduction in T_g . Thus, there seems to be no physically reasonable correlation between stability and mobility, at least using $T-T_g$ as a measure of mobility.

To further explore the relationship between the chemical reactivity and molecular mobility in the CEF mixtures the molecular mobility of CEF alone and in the mixtures was measured using isothermal microcalorimetry. The thermal activity of the CEF and the CEF mixtures was qualitatively similar to the data shown for the cephalosporins in Fig. 2, with a stretched kinetics curve that approached a nearly constant heat output at later times. The data for cefoxitin and

Table II. The Heat Capacity Change at T_g (ΔC_p) and Glass Transition Temperatures (T_g) for the Amorphous Drugs, Excipients and Mixtures in Used in this Study

Material	ΔC_p (J/g °C) (±0.1 J/g °C)	T_g (±0.1), °C
Cefamandol sodium	–	124
Cephalothin sodium	–	114
Cefoxitin sodium (CEF)	0.30	127
Sodium ethacrynate (ECA)	–	68 ^a
Sucrose	0.54	74
PVP k12	0.23	98
Trehalose	0.56	114
CEF:sucrose (1:10)	0.65	75
CEF:sucrose (1:3)	0.60	79
CEF:trehalose (1:10)	0.52	114
CEF:trehalose (1:3)	0.51	114
ECA:sucrose (1:10)	0.60	72
ECA:sucrose (1:3)	0.58	71
ECA:PVPk12 (1:10)	0.32	90
ECA:PVPk12 (1:3)	0.45	84
ECA:trehalose (1:10)	0.67	103
ECA:trehalose (1:3)	0.59	94

^a Estimated from the concentration dependence for T_g for various mixtures. The standard deviation in this estimate is ±3°C.

Table III. Relaxation Time Constants for Sucrose, Trehalose and PVP Measured Using Isothermal Microcalorimetry. The Standard Deviation in τ_D^β is Shown in Parenthesis Next to Each Value of τ_D^β

Temperature (°C)	Sucrose		Trehalose		PVP	
	τ_D^β , h	SD	τ_D^β , h	SD	τ_D^β , h	SD
40	14.1	2.2	79.0	33.4	25.5	2.2
40	10.0 ^a		33.4 ^a			
50	3.3	0.5	25.9	6.4	8.4	1.0
60	1.5	0.2	13.3	1.8	4.7	2.9
70	0.4 ^b		11.29	0.95	1.9 ^b	

^a Ref Liu and Pikal, 2002

^b Estimated using method of Shamblin *et al.* 1999 (6)

the mixtures were fit using the power-time form of the MSE equation that is appropriate for glassy systems undergoing chemical degradation (Eq. 7). The stretched enthalpy relaxation times for the cefoxitin systems are shown in Table I where they can be compared to the degradation times at the same temperatures as measured by HPLC. The limiting power values, P_k , which reflect the chemical degradation of CEF, showed the same trends as the $T_{10\%}$ values reported in Table I. These values were not reported due to the large errors associated with P_k term obtained by fit of Eq. 7 to the isothermal microcalorimetry data. Comparison of the τ_D^β values to the $T_{10\%}$ values shows no correlation whatsoever between the rate of chemical degradation of CEF and molecular mobility. While sucrose does indeed increase the mobility of cefoxitin as determined from the thermal data, it increases the stability.

Cefoxitin Sodium (CEF)–Additive Interactions

One important assumption critical to the notion that different materials will influence the chemical stability by moderating the molecular mobility is that the two components are present in the same amorphous phase. It has been shown that in general some degree of interaction between two components is necessary for miscibility to occur (30,31). Assuming that sucrose and drug are indeed present in a single amorphous phase, a possible explanation for reduced chemical reactivity in mixtures with sucrose may be that molecular interactions formed between the drug and sucrose when they are mixed inhibit chemical degradation. Some evidence for miscibility between sucrose and drug is indicated by the differences in the T_g values of the mixtures and drug alone (Table II) as well as the impact on chemical stability. One approach that has been used by Professor Zografis and co-workers to assess the degree of molecular interaction between two components in a miscible amorphous mixture is to compare the T_g of mixture to what is expected assuming that mixing is ideal. This comparison is made for the CEF mixtures containing sucrose and trehalose in Fig. 4 using the Gordon Taylor equation to predict the T_g of the mixtures, $T_{g,m}$,

$$T_{g,m} = \frac{w_1 T_{g1} + K w_2 T_{g2}}{w_1 + K w_2} \quad (13)$$

where w_i and T_{g_i} represents the weight fraction and T_g values, respectively, of each component in the mixture and K is the

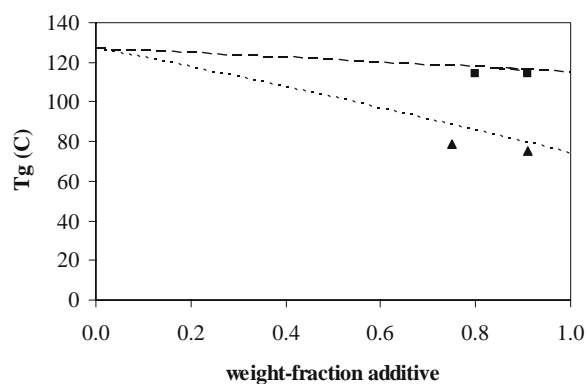


Fig. 4. The glass transition temperatures of CEF mixtures. The T_g values of mixtures were measured using DSC: sucrose (▲), trehalose (■). Lines represent T_g values predicted using the Gordon–Taylor equation for the sucrose mixtures (dotted line) and trehalose mixtures (dashed line).

ratio T_{g2}/T_{g1} . The T_g values for the sucrose and trehalose mixtures at both the 1:3 and 1:10 compositions are slightly lower than predicted from the Gordon–Taylor, although the sucrose mixtures deviate more than the trehalose mixtures. Unfortunately this analysis does little to explain the better stabilization of sucrose over trehalose, if the greater deviation in the sucrose mixtures compared to the trehalose mixtures is attributed to a less favorable degree of interaction (positive enthalpy of mixing).

Raman spectroscopy was used to look for molecular interactions between CEF and sucrose and trehalose that might explain the unexpected stabilizing effect that sucrose has on CEF and that would confirm miscibility the trehalose mixture. Raman spectra of amorphous cefoxitin alone and in the presence of sucrose and trehalose are shown in Fig. 5. The region of the spectrum shown covers the characteristic frequency range for C=O and C=C functionalities. Cefoxitin contains both of these functional groups while the sugars do not (the reference spectra of the amorphous sugars have no peaks in this region). It can be seen from Fig. 5, that there are two peaks in this region. The peak at approximately $1,641 \text{ cm}^{-1}$ in pure cefoxitin is shifted to a higher wavenumber when the material is freeze-dried with either trehalose ($1,645 \text{ cm}^{-1}$) or sucrose ($1,647 \text{ cm}^{-1}$). The peak at $1,769 \text{ cm}^{-1}$ is shifted very marginally in both trehalose and sucrose. These shifts indicate that the environment of certain cefoxitin functional groups is altered in the presence of the sugars confirming some degree of molecular level mixing. Since the sugars are most likely interacting with the carbonyl functions, the shift of peak 1 to a higher wavenumber in the presence of the sugars is indicative of a hydrogen bonding interaction between a sugar hydroxyl group and a cefoxitin carbonyl which is slightly weaker than the interaction found in pure amorphous CEF. This slightly weaker hydrogen bond interaction between CEF and additive relative to those in CEF alone suggests that miscibility is driven by the entropy gain associated with mixing. This shift supports the conclusion of miscibility of CEF with both trehalose and sucrose in the amorphous state. Since the carbonyl peak position (peak 1) is similar for sucrose and trehalose mixtures, the interactions between disaccharide and cefoxitin seem to be similar for both saccharides, and therefore, these data do not

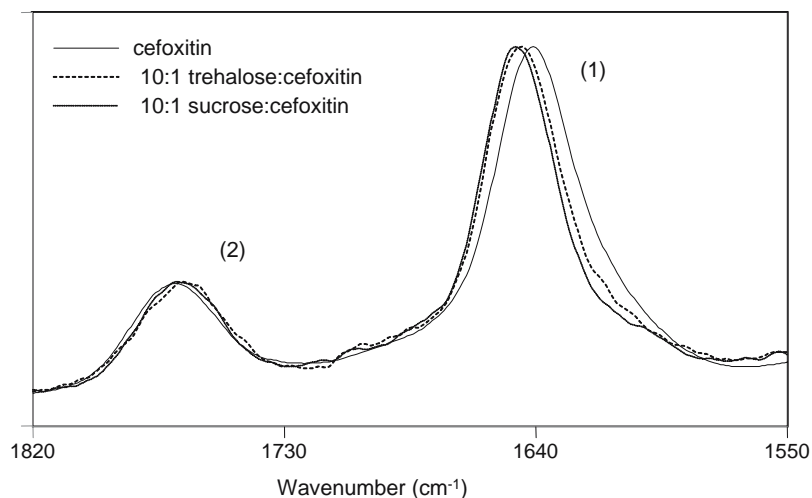


Fig. 5. Raman spectra of CEF alone and in 1:10 (CEF:additive) mixtures with trehalose and sucrose mixtures.

offer an obvious explanation for superior stabilization by sucrose relative to stabilization by trehalose.

Chemical Stability of Ethacrynate Sodium (ECA) Mixtures

When freeze-dried alone, ethacrynate sodium could not be prepared in the amorphous form due to spontaneous crystallization. Therefore, the chemical stability of ECA in the amorphous state could only be studied in mixtures with sucrose, trehalose and PVPK12. When ECA was lyophilized with sucrose, trehalose and PVP amorphous mixtures were produced as indicated by the absence of birefringence when examined by light microscopy. All of the mixtures showed a single glass transition that was intermediate between that of the additive and the estimated T_g value for ECA obtained by extrapolation of the T_g values of the mixtures (see later

discussion). Thus, the single T_g values for the mixtures were taken as an indication that the drug was miscible with each of the additives. The formation of a miscible amorphous mixture between ECA and the additives is also supported by the stabilization of ECA in the amorphous state (32).

Storage of ECA mixtures at 50, 60 and 70°C resulted in a decrease in drug concentration and a corresponding increase in the concentration of a single degradation peak detected using HPLC. This degradation peak, which elutes at a relative retention time of 2.4, has been assigned to a dimer of ethacrynic acid which is formed via a Diels–Alder type condensation (33). This ethacrynic acid dimer (ECA dimer) has been reported previously as the primary degradation mechanism in concentration solutions at neutral pH and in the amorphous state of both the ECA and the free acid form (33–35).

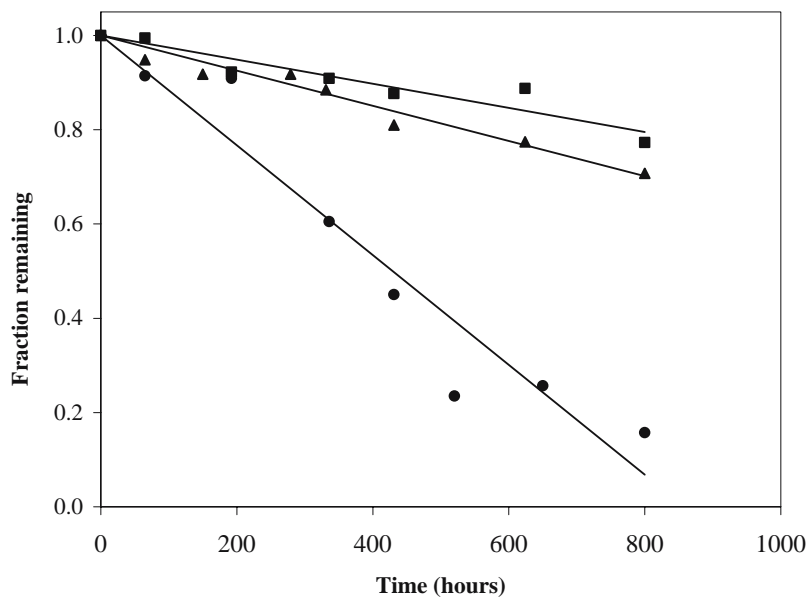


Fig. 6. Degradation of ECA at 60°C in 1:10 mixtures containing sucrose (●), trehalose (■) and PVP (▲). The error associated with the fraction remaining is no greater than the size of the symbols (i.e., no greater than 1%).

Table IV. Apparent Zero-Order Degradation Rate Constants and Time Required for 10% Degradation ($T_{10\%}$) for ECA Mixtures at 50, 60, and 70°C

Mixture	50°C			60°C		70°C	
	k (h^{-1})	$T_{10\%}$ (h)	τ_D^β (h)	k (h^{-1})	$T_{10\%}$ (h)	k (h^{-1})	$T_{10\%}$ (h)
ECA:sucrose 1:10	0.00028	364	4.3	0.00116	86	0.00682	15
ECA:sucrose 1:3	0.00018	543	5.8	0.00070	144	0.00474	21
ECA:trehalose 1:10	0.00013	769	28.4	0.00025	397	0.00124	81
ECA:trehalose 1:3	0.00023	437	17.1	0.00041	246	0.00288	35
ECA:PVP 1:10	0.00014	699	8.1	0.00035	290	0.00127	79
ECA:PVP 1:3	0.00019	518	11.8	0.00039	256	0.00122	82

The stretched enthalpy relaxation time τ_D^β (hours) is also reported for the ECA mixtures at 50°C. The RSD for $\tau_D^\beta(\text{Exp})$ is 10–15%.

The rate of transformation of ECA to the dimer was dependent on the additive mixed with ethacrynate sodium and increased with temperature, as expected, in all of the mixtures. An example of the loss of drug concentration due to dimer formation as a function of time for the 1:10 drug:excipient mixtures at 60°C is shown in Fig. 6. At a fixed ratio of additive to drug, the rate of conversion to dimer increased in the order trehalose < PVP < sucrose. These same trends were observed at all three temperatures for 1:3 drug:excipient mixtures. The rates of ECA loss due to dimer formation are compared for all of the mixtures at 50, 60 and 70°C in Table IV. For the reasons described previously, only initial degradation rates were of interest in this work.

The rate of dimer formation was constant in all the mixtures, and proceeded to nearly completion (80–90%) in some cases. This constant rate of dimer formation was unexpected for a mechanism that requires diffusion of large portions of the molecule and therefore, should slow down as the number of monomer units decreases. The observed kinetics can be explained by transfer of water from the vial stopper to the samples during storage. For those samples stored at the longest times at each temperature the water contents increased from 0.3 to 1–2% by weight. Thus, while the rate of dimer formation might normally be expected to slow down as monomer is consumed, or perhaps to follow 'stretched time kinetics' as do typical amorphous solids, the increased moisture content would be expected to lower T_g , increase molecular mobility, and thereby increase the reaction rate. The net effect is apparent 'zero-order' kinetics, but since we employ initial reaction rates, this effect is an annoyance rather than a serious problem.

In systems containing high level of 'stabilizer' (1:10 mixtures), the rate of ECA conversion to dimer is much faster in mixtures containing sucrose than in those containing either trehalose or PVP at all temperatures. For the sucrose mixtures, the addition of sucrose appears to promote dimer formation since the $T_{10\%}$ values decrease as the concentration of sucrose increases from 1:3 to 1:10 ECA:sucrose, for all temperature studied. In contrast increasing the amount of either PVP or trehalose increases the $T_{10\%}$ for dimer formation suggesting these additives inhibit the reaction. For mixtures containing trehalose or PVP, the rates of dimer formation are not greatly different, although trehalose appears to afford somewhat more stabilization than PVP at higher additive concentrations (i.e., 1:10 ECA:additive).

The increase in reaction rate with increasing sucrose concentration is likely due to the high degree of mobility in sucrose-rich mixtures where T_g values of the system are significantly lowered by sucrose. The opposite is true for increasing levels of trehalose and PVP mixtures where increasing levels of additive increase T_g and lead to improved ECA stability. For chemical reactions that require translational diffusion, such as dimer formation, Chang *et al.* (10) propose that in mixtures the observed reaction rate to some extent will be a consequence of a dilution effect. The model outlined by Chang *et al.* (10), suggests that reaction rate in a mixture relative to the pure state will be proportional to the volume fraction of that component. A critical assumption in this model is that whole molecule diffusion (diffusion over a length scale equal to the dimension of one molecule) is not possible due to the degree of immobilization in the system. The application of this model to glasses is justified since typically diffusion of entire molecules does not occur due to the restricted degree of molecular motion. Examination of the of the degradation data for the ECA mixtures at 50°C, where the glass dynamics are most likely to dominate (Table IV)

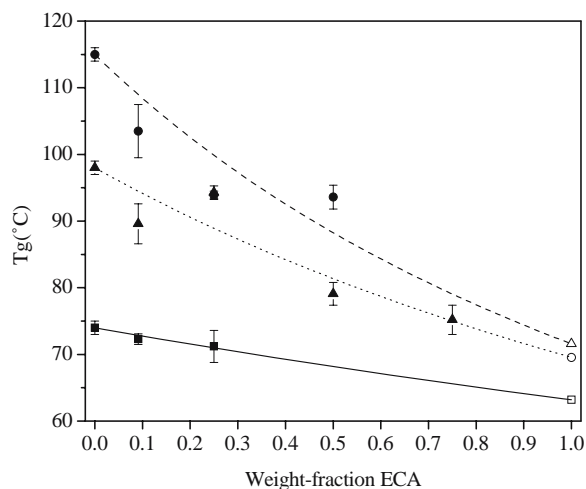


Fig. 7. Glass transition temperatures (T_g) for ECA mixtures containing sucrose (●), trehalose (■) and PVP (▲). The lines represent fit of the Fox equation to the experimental data using a nonlinear regression to determine a T_g for ECA that provides best fit to the data. The estimated T_g obtained for each mixture system is shown as an open symbol. The T_g of ECA taken as the average of the three values shown in the plot below is $68 \pm 3^\circ\text{C}$.

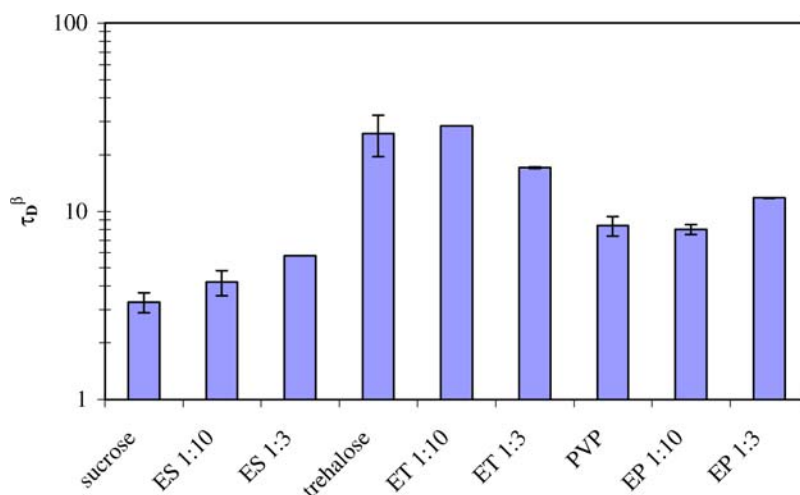


Fig. 8. Comparison of the τ_D^β values for ECA mixtures to the values for the additives alone at 50°C.

shows that the increase in stability with increasing trehalose and PVP is qualitatively consistent with some dilution effect. Assuming, as did Chang *et al.* (10), that drug weight-fraction approximates drug volume-fraction in the ECA mixtures, increasing the additive concentration from 1:3 to 1:10 is expected to decrease the reaction rate by a factor of 2.7. The observed effect is less than expected from this model for mixtures containing PVP and trehalose (i.e., reduction by only a factor of 1.4 and 1.9, for PVP and trehalose, respectively). It is possible in this case segmental or partial molecule diffusion, which are motions that are not excluded in this model, may be sufficient to allow dimer formation between two ECA molecules. Thus, the concentration effects seen in the trehalose and PVP mixtures, combined with differences in the rates that depend on which additive is present suggests that the effect of the additive on the reaction rate of ECA is a combination of an effect of molecular mobility and a dilution effect.

Molecular Mobility in Ethacrynate Sodium (ECA) Mixtures

The structural relaxation times for each of the mixtures were measured, or estimated from the τ_D^β values for the additives. From the T_g and τ_D^β values for the additives alone, the relaxation times of the ECA mixtures relative to one another is expected to increase a function of additive in the order: sucrose < PVP < trehalose, with mobility decreasing as relaxation time increases. However, whether the presence of the additive would increase or decrease the mobility of ECA could not be directly determined since an amorphous form of ECA could not be isolated. However, the T_g of pure ECA could be estimated. The T_g of ECA alone was estimated from the T_g values of the ECA-additive mixtures that produced a single T_g and showed no evidence of ECA crystallization. The T_g values for all of the ECA mixtures are shown in Fig. 7 as a function of composition. The Fox equation,

$$\frac{1}{T_{g_m}} = \frac{w_1}{T_{g_1}} + \frac{w_2}{T_{g_2}} \quad (14)$$

relates the T_g of a mixture, T_{g_m} , to the pure component T_g values and weight fractions, w , of the components present in

the mixture (36). The Fox equation was fit to the T_g values for the ECA mixtures using a nonlinear least-squares method using a T_g value for ECA that produced the best fit to the data. The average of the three T_g values obtained for ECA alone using the Fox equation describe the T_g of the mixtures, shown as the lines in Fig. 7, is $68 \pm 3^\circ\text{C}$ which is reported in Table II.

A comparison of the T_g values of sucrose, PVP and trehalose to the estimated T_g of ECA suggest that sucrose would only slightly increase T_g when mixed with ECA, while PVP and trehalose would produce a much larger increase in T_g . The measured T_g values for the ECA mixtures shown in Table II confirm the expected effect of each of the additives on a T_g of ECA that is 68°C . In strong contrast to the CEF systems, the chemical reactivity in the ECA mixtures, which is summarized in Table IV, does correlate with the T_g values for the mixtures. ECA mixtures containing PVP and trehalose, which have higher T_g values than the sucrose mixtures, show slower degradation rates and higher $T_{10\%}$ values.

Coupling between the chemical reactivity in the ECA mixtures and structural relaxation was examined by plotting $T_{10\%}$ versus τ_D^β for the mixtures at 50°C, as given in Table IV. As shown in Fig. 8, at a fixed additive concentration, the τ_D^β for the ECA mixtures increases in the order: sucrose < PVP < trehalose, which correlates with the rates of degradation as indicated by the $T_{10\%}$ values. A comparison of the τ_D^β values for the mixtures to the τ_D^β values for the additives alone shows that the mixtures containing sucrose have greater mobility than sucrose alone, whereas the mobilities in mixtures with PVP and trehalose are not greatly different than the mobilities of the pure additives. Thus, in contrast to the CEF system, ECA dimer formation at 50°C appears to be correlated to structural relaxation and molecular mobility in the glass. The extent to which these two processes are coupled is further examined in the discussion section below.

DISCUSSION

For two glassy cephalosporin drugs a rough correlation between rates of chemical reactivity and structural relaxation

supports the hypothesis that motions that contribute to structural relaxation are critical to chemical change. This hypothesis was tested further by studying the effects of temperature and the presence of a miscible additive on the chemical stability and molecular mobility of another cephalosporin drug, cefoxitin sodium. While the data are consistent with a correlation between structural relaxation and chemical stability in pure cefoxitin systems, this correlation was not maintained in the mixtures with sucrose and trehalose.

Degradation rates and τ_D^β values for pure cephalosporin systems (i.e., no additives present) were compared using data for CEF alone at two different temperatures, and data for the cefamandole and cephalothin systems. This comparison of the pure cephalosporins allowed an estimate of coupling between reactivity and mobility in glassy cephalosporin drugs that share a similar degradation mechanism. In Fig. 9, the degradation time ($T_{10\%}$) plotted *versus* the structural relaxation time constant τ_D^β , illustrates the correlation between structural relaxation time and the reaction time ($T_{10\%}$). The slope of the 'best fit' line through the data is equal to 0.55 and gives a coupling constant of ~ 0.25 indicating that the motions required for chemical degradation in the cephalosporins are weakly coupled to the motions involved in structural relaxation. Although chemical degradation in cephalosporins can be described generally in terms of reactivity of the β -lactam ring, the requirements for motions at the molecular level may not be exactly the same in all three drugs, and in the case of CEF, more than one reaction pathway is known to exist. Given that the analysis of structural relaxation is based on a macroscopic measure of the poorly understood changes taking place, the degree of coupling suggested by a coupling constant of 0.25 is rather good.

It has been shown that certain molecular motions are not closely coupled with viscosity and T_g , which, like τ_D^β are bulk measures of mobility on a relatively long length scale and long time scale (37–39). Indeed, recent evidence (40) suggests that at least well below T_g it may be fast dynamics, which are not represented by the enthalpy changes measured during structural relaxation, that are most highly correlated with stability. The τ_D^β obtained from measuring a change in a bulk property (enthalpy) with time is likely to represent an

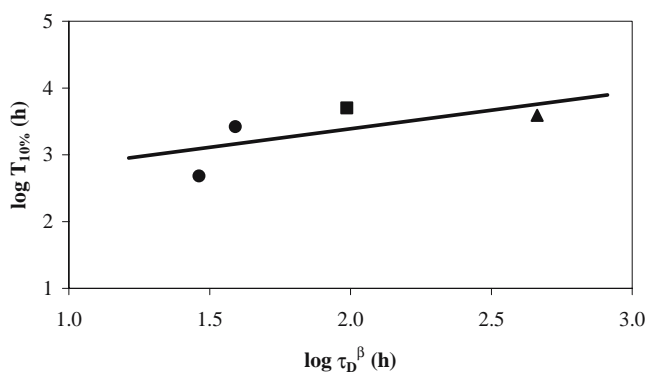


Fig. 9. Relationship between chemical reactivity ($T_{10\%}$ from HPLC) and molecular mobility (τ_D^β) for CEF (●), cephalothin (■) and cefamandole (▲). The τ_D^β were obtained from data plotted in time units of hours. The slope of the line of best fit through the data is ~ 0.55 with r^2 is equal to 0.42, and gives a coupling constant, c , equal to 0.25.

average time constant that is characteristic of many motions that contribute to glass dynamics. While this work does not, in itself, provide sufficient information to allow structural relaxation rates to be quantitatively predictive of reaction rates in glassy cephalosporin drugs, it does provide a point of reference for future studies. We suggest that with additional study, it might be possible to establish coupling of chemical reactivity and molecular mobility in glasses in general and more specifically in drugs with degradation mechanisms that may be similar (i.e., ring opening via hydrolysis) or different (dimer formation, acid–base).

The lack of correlation between degradation rate and molecular mobility in the CEF mixtures suggests that the simple relationship between reactivity and molecular mobility implied by Eqs. 4 and 5, with a constant coupling coefficient, may be inadequate to account for the more complex molecular dynamics in the CEF mixtures. The coupling coefficient may vary with composition and when molecular motions other than those measured by structural relaxation time are critical. While it is possible that the molecular motions of the individual components will be well represented by a single τ_D^β for the mixture, it is also possible that using a single relaxation time to describe the mobility of all components is an oversimplification. A single time constant to describe the mobility of all components would require the components to have strong molecular interactions and complete coupling of the motions of one component to one another. Even in miscible systems interactions present between like molecules (i.e., aa, bb) will prevent complete coupling of molecular motions between two unlike components (i.e., ab) (30,31). Further, it has been shown that the molecular motions of the individual components in a miscible systems are often not completely coupled (37,39).

Another important observation of this work is the ability of sucrose to provide stabilization, which could not be attributed to specific interaction between CEF and sucrose given the similarity of Raman spectra in sucrose and trehalose formulations. There are several examples in the literature where sucrose was found to stabilize proteins in a manner that is unexpected, either because the addition of sucrose to a protein has lowered the T_g and yet has effectively stabilized the protein (10,41); or because other saccharides produce a greater reduction in mobility but yet do not stabilize as well as does sucrose (12). This study shows, for the first time, that sucrose can also stabilize low molecular weight amorphous drugs in an 'anomalous' fashion. The rationalization of such behavior in terms of subtle conformational changes that was used to explain protein stabilization

Table V. Calculated Enthalpy Relaxation Time Constants (τ^β) for ECA Mixtures at 60 and 70°C Based on Values at Determined at 50°C from Isothermal Microcalorimetry τ_D^β

Mixture	$d \ln \tau_D^\beta / dT/T_g$	50°C τ_D^β	60°C τ^β	70°C τ^β
ECA:sucrose 1:10	45	1.5	0.16	-1.2
ECA:sucrose 1:3	37.4	1.8	0.67	-0.41
ECA:trehalose 1:10	46.1	3.4	2.1	0.90
ECA:trehalose 1:3	31	2.8	2.0	1.2
ECA:PVP 1:10	17.8	2.1	1.6	1.1
ECA:PVP 1:3	20.5	2.5	1.9	1.3

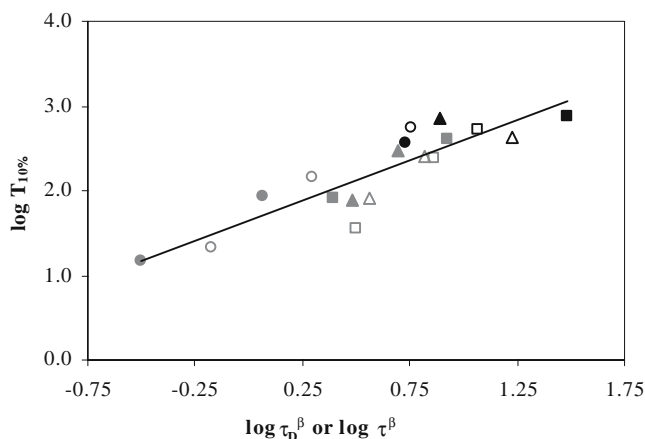


Fig. 10. Degradation times ($T_{10\%}$) of ECA in mixtures with sucrose (\bullet, \circ), trehalose (\blacksquare, \square) and PVP ($\blacktriangle, \triangle$) plotted versus structural relaxation times. Closed symbols indicate 1:10 mixtures and open symbol indicated 1:3 mixtures. Relaxation times measured at 50°C using isothermal microcalorimetry (τ_D^β) are shown as dark symbols and calculated relaxation times (τ^β) at 60 and 70°C are shown as light (grey) symbols. The slope of the line of best fit through the data is ~ 0.95 with r^2 is equal to 0.79, and gives a coupling constant, c , equal to 0.43.

cannot be the explanation. The point of significance is that if sucrose can stabilize small molecules where conformational issues can not be responsible, why would we assume the effect of sucrose on protein stability must have its origin in structural effects? Recent reports in the literature suggest that ability of an additive to improve the chemical stability or biological activity of a protein may be due to the effect on more subtle molecular motions that may not be reflected by T_g , or even the motions measured during structural relaxation (9,40). That is, high frequency, low amplitude motions, or ‘fast dynamics’ may control differences in stability between formulations at temperatures well below T_g . This effect while not well understood on a mechanistic level is supported by significant empirical evidence (9,40).

In contrast to the CEF mixtures, the rate of ECA dimer formation in the ECA mixtures appears to correlate reasonably well to τ_D^β values, at least at 50°C. The coupling of ECA dimer formation to structural relaxation was determined using τ_D^β values obtained for the ECA mixtures at 50°C and relaxation times at 60 and 70°C. The relaxation times at 60 and 70°C, reported in Table V, were calculated from Eq. 6 using τ_D^β at 50°C, the experimental values of T_g and ΔC_p for the mixtures (shown in Table II) and width of the glass transition temperature (shown in Table V). The calculated relaxation times at 60 and 70°C are compared to those measured at 50°C in Table V.

The rates of ECA dimer formation in the various formulations are compared to the structural relaxation time constants in Fig. 10, using the data in Table V. For the ECA mixtures the correlations are relatively good, with nearly 80% of the variation consistent with variation in mobility. Note that one cannot expect a perfect correlation both because the errors in the data are significant and because a comparison such as that given in Fig. 10 assumes all systems have the same coupling coefficient. Moreover, as one can observe, the 1:10 systems normally have better stability than the corresponding 1:3 systems, even when compared at the

same ‘hypothetical’ τ^β . One might argue that this observation has its origin in the ‘dilution effect’, and because of the dilution effect, a comparison of rate constants with mobility should employ rate constants where the dilution effect has been eliminated. That is, perhaps one should compare the values of k_0 ($=k/X_d$, X_d =weight fraction of drug) with mobility. A plot similar to Fig. 10 except using k_0 gives a nearly identical correlation coefficient and a similar overall appearance. However, with the k_0 correlation the rate constants for the 1:10 formulations are now systematically higher than the corresponding 1:3 systems. That is, the simplified dilution effect suggested in the literature seems to ‘overcorrect’ for variation in level of excipient, at least in the systems studied.

The slope of the ‘best fit’ line drawn through data in Fig. 10 is equal to 0.95 and gives a coupling constant, c , of 0.43, indicating the coupling for the ECA systems is relatively strong. Since ECA dimer formation requires translational diffusion of large portions of the ECA molecule, it is perhaps not surprising that this reaction correlates more closely to structural relaxation than the does the process of β -lactam ring opening in the CEF molecule, the latter likely requiring motion on a shorter (molecular) length scale than whole molecule diffusion. These results suggest that structural relaxation rates may be predictive of chemical changes that require diffusion over long (molecular) length scales.

CONCLUSIONS

In this study coupling of chemical degradation to glass dynamics was shown to be relatively strong (coupling coefficient, $c \sim 0.43$) for ECA dimerization, for which diffusion over molecular length scales is required. In contrast, the degradation of cephalosporin drugs, which degraded primarily via a hydrolysis of the β -lactam ring, were only weakly coupled (coupling coefficient, $c \sim 0.25$). This result suggests that chemical degradation, which involve mobility over short (molecular) length scales are not as strongly coupled to structural relaxation time constants. For one of the cephalosporin drugs, cefoxitin sodium, no correlation between the rates of chemical degradation and structural relaxation was evident in mixtures. This lack of correlation was due in part to an unexpected stabilizing effect by sucrose despite increased mobility. The stabilization could not be attributed to specific interactions. This observation suggests that motions governing the rate controlling step in chemical degradation can be different from those associated with structural relaxation, particularly in mixtures. To better understand the complex relationship between molecular mobility in amorphous systems and the chemical reactivity, additional techniques that can detect the molecular motions of specific functional groups and/or measure motions with time scale ranging over several decades at a single temperature are required.

ACKNOWLEDGMENTS

The authors are grateful to Merck Frosst Canada for providing the financial support for a postdoctoral fellowship for SLS. Professor Lynne Taylor is acknowledged for performing Raman spectroscopy experiments and interpre-

tation of the data for the objectives of this work. The authors also acknowledge Dr. Xiaolin Tang for his assistance in performing isothermal microcalorimetry experiments in support of this work. The discussions with Professor George Zografu were helpful in bringing understanding to this topic.

REFERENCES

1. E. R. Oberholzer and G. S. Brenner. Cefoxitin sodium: solution and solid state chemical stability studies. *J. Pharm. Sci.* **68**:836–866 (1979).
2. M. J. Pikal and K. M. Dellerman. Stability testing of pharmaceuticals by high-sensitivity isothermal calorimetry at 25°C: cephalosporins in the solid and aqueous solution states. *Int. J. Pharm.* **50**:233–252 (1989).
3. J. Li, Y. Guo, and G. Zografu. The solid-state stability of amorphous quinapril in the presence of beta-cyclodextrins. *J. Pharm. Sci.* **91**:229–243 (2002).
4. B. C. Hancock, S. L. Shamblin, and G. Zografu. The molecular mobility of amorphous pharmaceutical solids below their glass transition temperatures. *Pharm. Res.* **12**:799–806 (1995).
5. K. Kawakami and M. J. Pikal. Calorimetric investigation of the structural relaxation of amorphous materials: evaluating validity of the methodologies. *J. Pharm. Sci.* **94**:948–965 (2005).
6. S. L. Shamblin, X. Tang, L. Chang, B. C. Hancock, and M. J. Pikal. Characterization of the time scales of molecular motion in pharmaceutically important glasses. *J. Phys. Chem., B* **103**:4113–4121 (1999).
7. M. C. Lai, M. J. Hageman, R. L. Schowen, R. T. Borchardt, and E. M. Topp. Chemical stability of peptides in polymers. 1. Effect of water on peptide deamidation in poly(vinyl alcohol) and poly(vinyl pyrrolidone) matrices. *J. Pharm. Sci.* **88**:1073–1080 (1999).
8. S. Yoshioka, Y. Aso, and S. Kojima. Temperature- and glass transition temperature-dependence of bimolecular reaction rates in lyophilized formulations described by the Adam–Gibbs–Vogel equation. *J. Pharm. Sci.* **93**:1062–1069 (2004).
9. M. T. Cicerone and C. L. Soles. Fast dynamics and stabilization of proteins: binary glasses of trehalose and glycerol. *Biophys. J.* **86**:3836–3845 (2004).
10. L. Chang, D. Shepherd, J. Sun, D. Ouellette, K. L. Grant, X. Tang, and M. J. Pikal. Mechanism of protein stabilization by sugars during freeze-drying and storage: native structure preservation, specific interaction, and/or immobilization in a glassy matrix?. *J. Pharm. Sci.* **94**:1427–1444 (2005).
11. B. S. Chang, R. M. Beauvais, A. Dong, and J. F. Carpenter. Physical factors affecting the storage stability of freeze-dried interleukin-1 receptor antagonist: glass transition and protein conformation. *Arch. Biochem. Biophys.* **331**:249–258 (1996).
12. S. P. Duddu and P. R. Dal Monte. Effect of glass transition temperature on the stability of lyophilized formulations containing a chimeric therapeutic monoclonal antibody. *Pharm. Res.* **14**:591–595 (1997).
13. C. A. Angell. Strong and fragile liquids. In K. I. Ngai and G. B. Wright (eds.), *Relaxation in Complex Systems*. National Technical Service, US Department of Commerce, Springfield, 1984, pp. 3–11.
14. M. D. Ediger, C. A. Angell, and S. R. Nagel. Supercooled liquids and glasses. *J. Phys. Chem.* **100**:13200–13212 (1996).
15. C. Angell. Relaxation in liquids, polymers and plastic crystals—strong/fragile patterns and problems. *J. Non-cryst. Solids* **131–133**:13–31 (1991).
16. M. J. Pikal. Mechanisms of protein stabilization during freeze-drying and storage: the relative importance of thermodynamic stabilization and glassy state dynamics. In L. Rey and J. C. May (eds.), *Freeze-drying/Lyophilization of Pharmaceutical and Biological Products, Vol. 96*, Drugs and the Pharmaceutical Sciences, Marcel Dekker, New York, 1999.
17. Y. Guo, S. R. Byrn, and G. Zografu. Physical characteristics and chemical degradation of amorphous quinapril hydrochloride. *J. Pharm. Sci.* **89**:128–143 (2000).
18. F. Fajara, B. Geil, H. Sillescu, and G. Fleischer. Translational and rotational diffusion in supercooled orthoterphenyl close to the glass transition. *Zeitschrift fuer Physik B: Condensed Matter* **88**:195–204 (1992).
19. C. A. Angell. Dynamic process in ionic glasses. *Chem. Rev.* **90**:523–532 (1990).
20. C. A. Angell, R. D. Bressel, J. L. Green, H. Kanno, M. Oguni, and E. J. Sare. Liquid fragility and the glass transition in water and aqueous solutions. *J. Food Eng.* **22**:115–142 (1994).
21. I. E. T. Iben, D. Braunstein, W. Doster, H. Frauenfelder, M. K. Hong, J. B. Johnson, S. Luck, P. Ormos, A. Schulte, P. J. Steinback, A. H. Xie, and R. D. Young. Glassy behavior of a protein. *Phys. Rev. Lett.* **62**:1916–1919 (1989).
22. S. P. Duddu, G. Zhang, and P. R. Dal Monte. The relationship between protein aggregation and molecular mobility below the glass transition temperature of lyophilized formulations containing a monoclonal antibody. *Pharm. Res.* **14**:596–599 (1997).
23. J. Liu, D. R. Rigsbee, C. Stotz, and M. J. Pikal. Dynamics of pharmaceutical amorphous solids: the study of enthalpy relaxation by isothermal microcalorimetry. *J. Pharm. Sci.* **91**:1853–1862 (2002).
24. A. Mangia, A. Scandroglio, S. Silingardi, and P. Del Buttero. High-performance liquid chromatographic analysis of cefoxitin and related chemical compounds. *Il Farmaco; edizione pratica* **41**:107–112 (1986).
25. G. S. Brenner. Cefoxitin, sodium. *Anal. Profiles Drug Subst.* **11**:169–195 (1982).
26. M. J. Pikal, L. Chang, and X. C. Tang. Evaluation of glassy-state dynamics from the width of the glass transition: results from theoretical simulation of differential scanning calorimetry and comparisons with experiment. *J. Pharm. Sci.* **93**:981–984 (2004).
27. M. Peyron, G. K. Peirens, A. J. Lucas, L. D. Hall, and R. C. Stewart. The modified stretched-exponential model for characterization of NMR relaxation in porous media. *J. Magn. Reson.* **118**:214–220 (1996).
28. S. L. Shamblin, B. C. Hancock, Y. Dupuis, and M. J. Pikal. Interpretation of relaxation time constants for amorphous pharmaceutical systems. *J. Pharm. Sci.* **89**:417–427 (2000).
29. E. M. Cohen. Polarographic determination of ethacrynic acid. *J. Pharm. Sci.* **60**:1702–1704 (1971).
30. S. L. Shamblin, L. S. Taylor, and G. Zografu. Mixing behavior of colyophilized binary systems. *J. Pharm. Sci.* **87**:694–701 (1998).
31. L. S. Taylor and G. Zografu. Sugar–polymer hydrogen bond interactions in lyophilized amorphous mixtures. *J. Pharm. Sci.* **87**:1615–1621 (1998).
32. S. L. Shamblin, E. Y. Huang, and G. Zografu. The effects of colyophilized polymeric additives on the glass transition temperature and crystallization of amorphous sucrose. *J. Therm. Anal.* **47**:1567–1579 (1996).
33. A. J. Phillips, R. J. Yarwood, and J. H. Collett. Thermal analysis of freeze dried products. *Anal. Proc.* **23**:394–395 (1986).
34. R. J. Yarwood, A. J. Phillips, and J. H. Collett. Processing factors influencing the stability of freeze dried sodium ethacrylate. *Drug Dev. Ind. Pharm.* **12**:2157–2170 (1986).
35. R. J. Yarwood, W. D. Moore, and J. H. Collett. Liquid chromatographic analysis of ethacrynic acid and degradation products in pharmaceutical systems. *J. Pharm. Sci.* **74**:220–223 (1985).
36. B. C. Hancock and G. Zografu. The relationship between the glass transition temperature and the water content of amorphous pharmaceutical solids. *Pharm. Res.* **11**:471–477 (1994).
37. M. T. Cicerone and M. D. Ediger. Enhanced translation of probe molecules in supercooled *o*-terphenyl: signature of spatially heterogeneous dynamics. *J. Chem. Phys.* **104**:7210–7218 (1996).
38. M. T. Cicerone, P. A. Wagner, and M. D. Ediger. Translational diffusion on heterogeneous lattices: a model for dynamics in glass forming materials. *J. Phys. Chem., B* **101**:8727–8734 (1997).
39. C. A. Oksanen and G. Zografu. Molecular mobility in mixtures of absorbed water and solid poly(vinylpyrrolidone). *Pharm. Res.* **10**:791–799 (1993).
40. M. T. Cicerone, C. L. Soles, Z. Chowdhuri, M. J. Pikal, and L. Chang. Fast dynamics as a diagnostic for excipients in preservation of dried proteins. *Am. Pharm. Rev.* **8**:22, 24–27 (2005).
41. L. Chang, D. Shepherd, J. Sun, X. Tang, and M. J. Pikal. Effect of sorbitol and residual moisture on the stability of lyophilized antibodies: implications for the mechanism of protein stabilization in the solid state. *J. Pharm. Sci.* **94**:1445–1455 (2005).